Molecular behaviour of elastomeric materials under large deformation: 2. Rheological model of polymer networks

Yoshihide Fukahori and Wataru Seki
Research and Development Division, Bridgestone Corporation, Kodaira-Shi, Tokyo 187, Japan
(Received 30 November 1990; revised 18 February 1991; accepted 11 March 1991)

The molecular mechanism of real rubber vulcanizates, both unfilled and filled, is discussed in relation to the classical non-Gaussian theory, in which the deviation from theory at large deformation seems to be attributable to the concept of fixed crosslinks in the theory. A new slider model that possesses the characteristic viscous property is introduced to represent physical crosslinks. The slider model is effectively available for interpreting the typical phenomena observed in real rubber vulcanizates, such as the crossing of the stress–strain curves measured at different temperatures and the Mullins softening under cyclic deformation.

(Keywords: rubber elasticity; molecular mechanism; deformation; non-Gaussian theory; slider model; stress–strain curve crossing; stress softening; Mullins effect)

INTRODUCTION

Numerous theories have been published over the past 10 to 20 years concerning the molecular structures of polymer networks and their elastomeric properties, most of which are a challenge to classical elasticity theory. More recently, in particular, there have been many heated discussions on the effects of chain entanglement between two crosslinks[1–10], where new synthetic techniques have become available for the preparation of controlled model networks of known structure such as hydroxyl-terminated polydimethylsiloxane[10].

In the previous paper[11], we considered rubber elasticity theories from the standpoint of a phenomenological approach and elucidated the characteristics of the strain energy function of various rubber vulcanizates under large deformation. In the present paper, we discuss the molecular structures of polymer networks in comparison with molecular theories. First, we show experimental results that the temperature dependence of the stress–strain relation is not constant but a function of strain amplitude, which is different from the result derived by the classical elasticity theories. It is necessary for understanding the above phenomena to consider unstable or unfixed crosslinks instead of the fixed crosslinks on which the theories are based. It is the purpose of this report to propose a new rheological model and analyse the molecular behaviour of elastomeric materials under large deformation. The characteristics of the molecular mechanism of chemical crosslinks, physical crosslinks and chain entanglement will be clearer in large, sometimes very large, deformations than in small ones. Rubber vulcanizates not idealized but generally used in industry are treated here with respect to both unfilled and filled natural rubber.

0032-3861/92/051058-11

THEORETICAL BACKGROUND

The classical molecular theories of rubber-like elasticity[12–15] are based on a Gaussian distribution function for the end-to-end distance of the network chains whose configuration in space is independent of each other. The crosslinks or junction points are assumed to be embedded in the network (fixed junction, then no fluctuation) and move affinely with any macroscopic deformation imposed on the elastomers.

The Gaussian theory gives the elastic free energy of deformation:

$$W = \tfrac{1}{2}\nu kT(\lambda_1^2 + \lambda_2^2 + \lambda_3^2 - 3) \qquad (1)$$

where ν is the number of network chains per unit volume (the crosslink density), k is Boltzmann's constant and λ is the extension ratio. For simple extension, the stress per unit deformation area is:

$$\sigma = \nu kT(\lambda - \lambda^{-2}) \qquad (2)$$

If the network junctions are allowed to fluctuate freely about their mean positions as recent works[16–18] suggest, the elastic free energy will be given by:

$$W = \tfrac{1}{2}A_\phi \nu kT(\lambda_1^2 + \lambda_2^2 + \lambda_3^2 - 3) \qquad (3)$$

where $A_\phi < 1$, i.e. junction fluctuations diminish the modulus by a factor A_ϕ compared with equation (1).

The classical theories of a purely entropic elasticity, represented by equation (1) or equation (3) lead to the brilliant conclusion that stress should be directly proportional to absolute temperature at constant λ. This is based on the assumption that the free-energy expression can be given in terms of the conformational entropy alone. In real elastomers, however, it is well known from thermodynamic considerations that,

although the energetic contribution cannot be completely negligible, the fraction of the energetic component in the elastic force, σ_e/σ, is only about 0.15 for natural rubber[19]. Kawabata *et al.*[20], according to their experiments at moderately large deformation, divided the total elastic energy into two independent terms. The first entropic term is exactly the same as equation (1) and the second energetic term is observed to be almost independent of temperature.

The non-Gaussian statistical theory derived by Kuhn and Grün[21] takes into account the finite extensibility of a single chain by using the inverse Langevin function $\mathscr{L}^{-1}$. The entropic elastic force of a single chain is given as:

$$\sigma = (kT/l)\mathscr{L}^{-1}(r/nl) \tag{4}$$

where n is the number of segments in the chain and l is the length of a segment. When we consider a rubber network consisting of ν chains and assume an affine deformation, the entropic force for uniaxial extension can be expressed, neglecting the energy contribution, as[22]:

$$\sigma = \frac{\nu kT}{3} n^{1/2}\left[\mathscr{L}^{-1}\left(\frac{\lambda}{n^{1/2}}\right) - \lambda^{-2/3}\mathscr{L}^{-1}\left(\frac{1}{\lambda^{1/2}n^{1/2}}\right)\right] \tag{5}$$

The most important feature of the theory is that it predicts a strong upturn at large extension, which is the direct consequence of the limited extensibility of chains as observed in real rubber-like materials. The non-Gaussian stress–strain relations are determined by two parameters, ν and n; the former defines the modulus in the region of small and moderate strain, and the latter controls the behaviour in the high strain region and the ultimate extensibility of the network. Since there is the following relation in crosslinked networks:

$$\nu M = \rho A$$

where ρ is the density of rubber, M is the average molecular weight of a network chain and A is Avogadro's number, and ρ is independent of extension because of the incompressibility of rubber, we can find the relation:

$$n\nu = \text{constant}$$

It is also shown that the stress given by equation (5) is proportional to absolute temperature and independent of the strain amplitude. Although the non-Gaussian theory is not necessarily a quantitative representation of rubber-like elasticity in which chain entanglements, energy contribution, non-affine deformation, etc. are not taken into consideration, it can be regarded as predicting the essential features of the stress–strain behaviour of real elastomeric materials. Anyway, all the theories discussed above clearly indicate that the stress increases linearly with absolute temperature, independent of the magnitude of extension ratio λ.

In the previous paper[11], we discussed the molecular behaviour of elastomers from the viewpoint of the continuum theory of finite deformation, where the stress–strain relation of elastomers can be derived from the strain energy function W, which is given as a function of strain invariants I_1 and I_2:

$$W = W(I_1, I_2) \tag{6}$$

Here

$$I_1 = \lambda_1^2 + \lambda_2^2 + \lambda_3^2$$

$$I_2 = \lambda_1^2\lambda_2^2 + \lambda_2^2\lambda_3^2 + \lambda_3^2\lambda_1^2$$

and λ_1, λ_2 and λ_3 are the principal extension ratios. In the case of uniaxial extension, considering $\lambda_1\lambda_2\lambda_3 = 1$ and $\lambda_2 = \lambda_1^{-1/2}$:

$$\sigma = 2(\lambda - \lambda^{-2})\left(\frac{\partial W}{\partial I_1} + \lambda^{-1}\frac{\partial W}{\partial I_2}\right) \tag{7}$$

According to our experimental results for various rubber vulcanizates, $\partial W/\partial I_1$ is the main part of the reduced stress $\sigma/2(\lambda - \lambda^{-2})$ and $\partial W/\partial I_2$ is negligibly small. Therefore, by considering the temperature-dependent properties of $\partial W/\partial I_1$ as a function of λ, we can understand the characteristics, in other words the limits of the classical elasticity theories, equation (2) and equation (5).

EXPERIMENTS

Experiments in strip biaxial and simple extension were performed at crosshead speeds of 50 mm min^{-1} over a wide range of temperatures from 24 to 120°C. The compounding details of the natural rubber (NR) vulcanizates used here were given in the previous paper[11], which roughly have the following characteristics: unfilled (NR2), slightly filled (NR5) and heavily filled (NR7) with carbon black.

RESULTS

Temperature dependence of the strain energy function

The temperature-dependent properties of the partial derivatives of the strain energy function, $\partial W/\partial I_1$ and $\partial W/\partial I_2$, in NR2 are shown in *Figure 1* as a function of strain invariant I_1 ($= I_2$ in strip biaxial). As the temperature increases, $\partial W/\partial I_1$ increases at small and

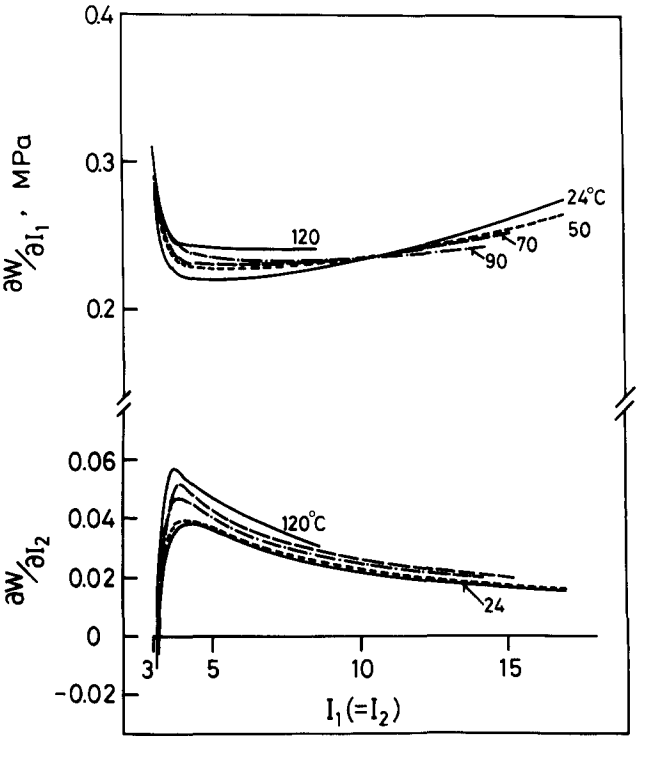

Figure 1 Temperature dependence of $\partial W/\partial I_1$ and $\partial W/\partial I_2$ as a function of I_1 for NR2

medium strain ($I_1 \simeq 3$–10) but decreases at large strain, which means that the curves of $\partial W/\partial I_1$ vs. I_1 at different temperatures cross each other. On the other hand, $\partial W/\partial I_2$ has higher value at higher temperature, independent of strain amplitude. These tendencies are also seen in a slightly filled NR (NR5), as shown in *Figure 2*. In a heavily filled NR (NR7), however, no crossing can been seen among the curves of $\partial W/\partial I_1$ vs. I_1 (*Figure 3*), where $\partial W/\partial I_1$ decreases rapidly with increasing temperature and $\partial W/\partial I_2$ is independent of temperature.

This temperature dependence of $\partial W/\partial I_1$ is represented in a different manner in *Figure 4* (NR2), *Figure 5* (NR5) and *Figure 6* (NR7) as a function of temperature at constant strain invariant I_1. It is clearly shown that $\partial W/\partial I_1$ increases at small extension but decreases at higher extension as the temperature increases in NR2 and NR5. This phenomenon is demonstrated more clearly in *Figure 7*, in which the temperature coefficient of $\partial W/\partial I_1$, $(\partial/\partial T)(\partial W/\partial I_1)$ is plotted against I_1 and λ for three rubber vulcanizates. The plot of $(\partial/\partial T)(\partial W/\partial I_1)$ has a positive value at small and medium extension in NR2 and NR5, which means that entropic force mainly governs the rubber elasticity of these materials. Even in such an extension region, however, $(\partial/\partial T)(\partial W/\partial I_1)$ is not constant but is a function of strain having a maximum value, following which it decreases gradually to a negative value as extension increases. It is the logical conclusion of classical elasticity theories, whether Gaussian or non-Gaussian, that stress increases in proportion to absolute temperature, independent of strain amplitude. Therefore, considering our experimental results in the previous paper[11] that $\partial W/\partial I_1$ is the main part of the stress and $\partial W/\partial I_2$ can be neglected, the situations derived above seem to demonstrate that these rubber vulcanizates change their elastic properties from entropic to energetic as the extension increases. In

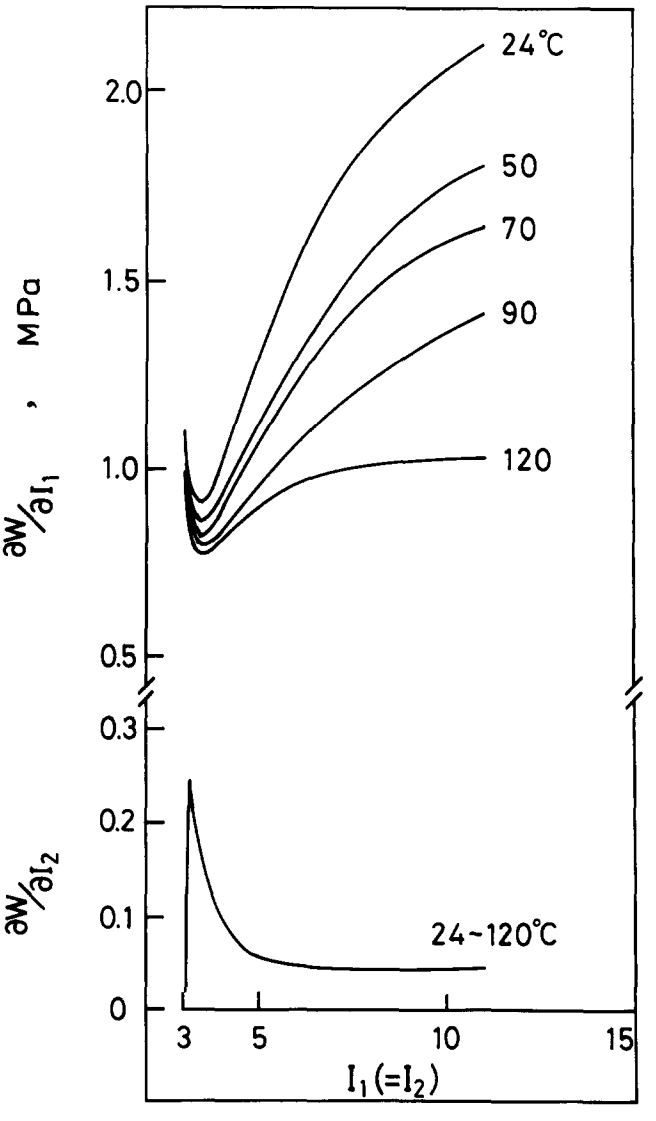

Figure 3 As *Figure 1* but for NR7

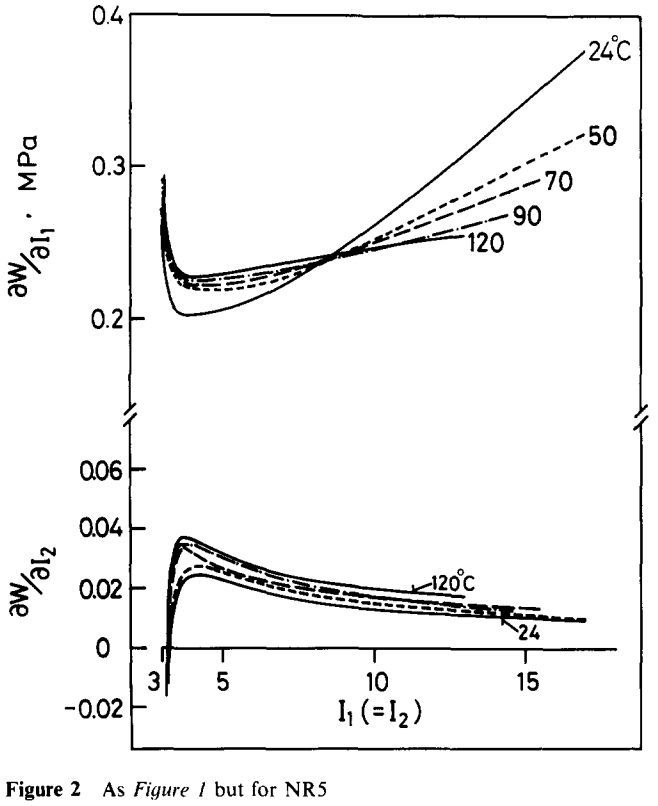

Figure 2 As *Figure 1* but for NR5

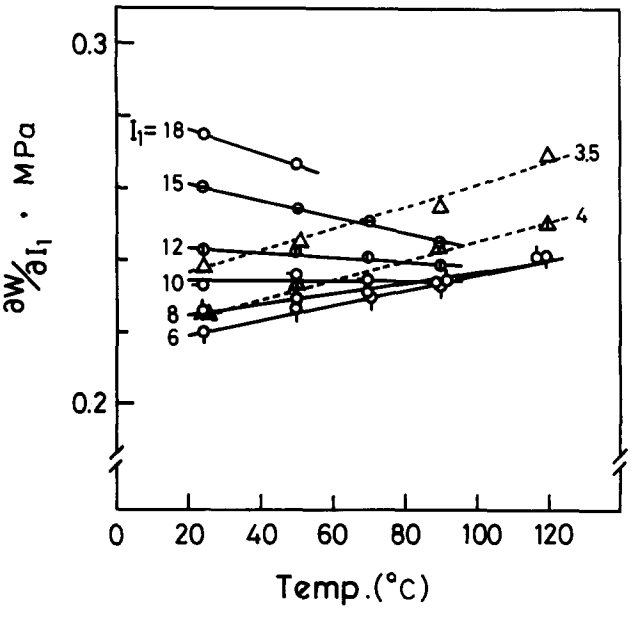

Figure 4 Plot of $\partial W/\partial I_1$ against temperature for NR2

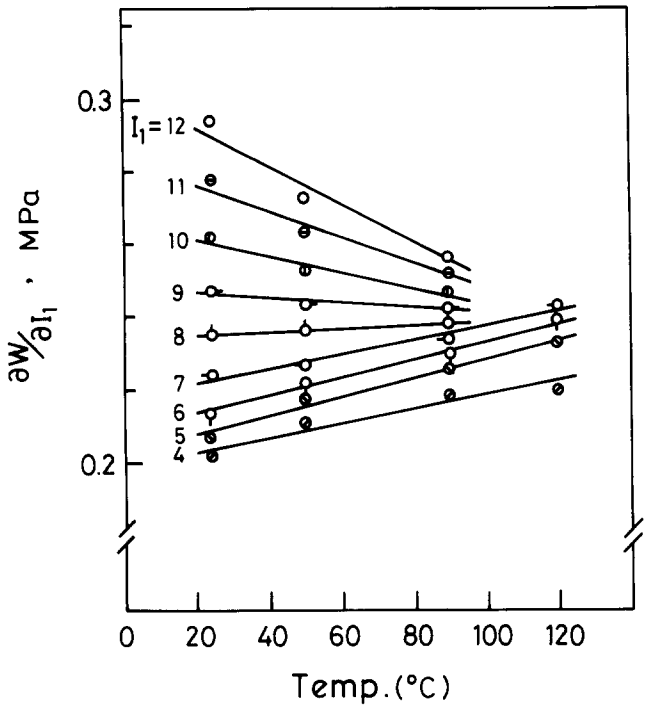

Figure 5 As *Figure 4* but for NR5

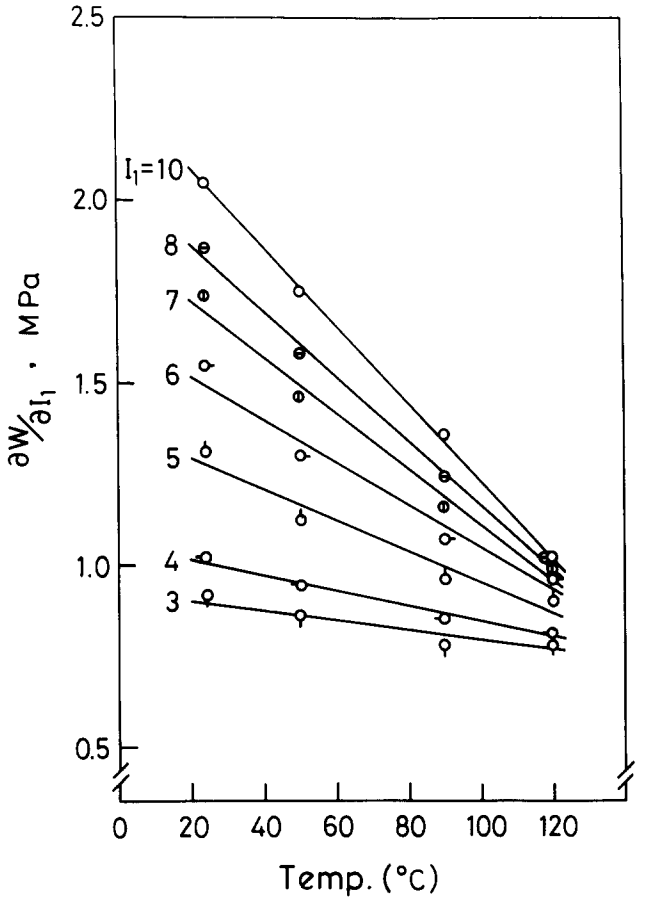

Figure 6 As *Figure 4* but for NR7

particular, a heavily filled NR only shows energetic behaviour, independent of strain amplitude. These situations are also clearly observed in the stress–strain relation in simple extension, as will be shown below.

Temperature dependence of the stress–strain relation in simple extension

Figure 8 shows the stress–extension ratio relations of NR2 measured in simple extension at various temperatures. The stress increases in the region of moderately

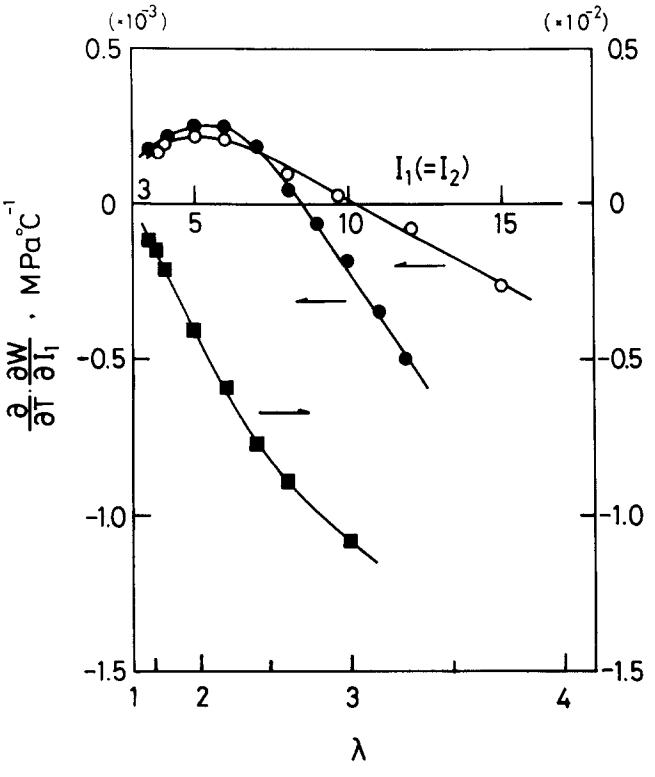

Figure 7 Temperature coefficient of $\partial W/\partial I_1$ as a function of I_1: (○) NR2, (●) NR5, (■) NR7

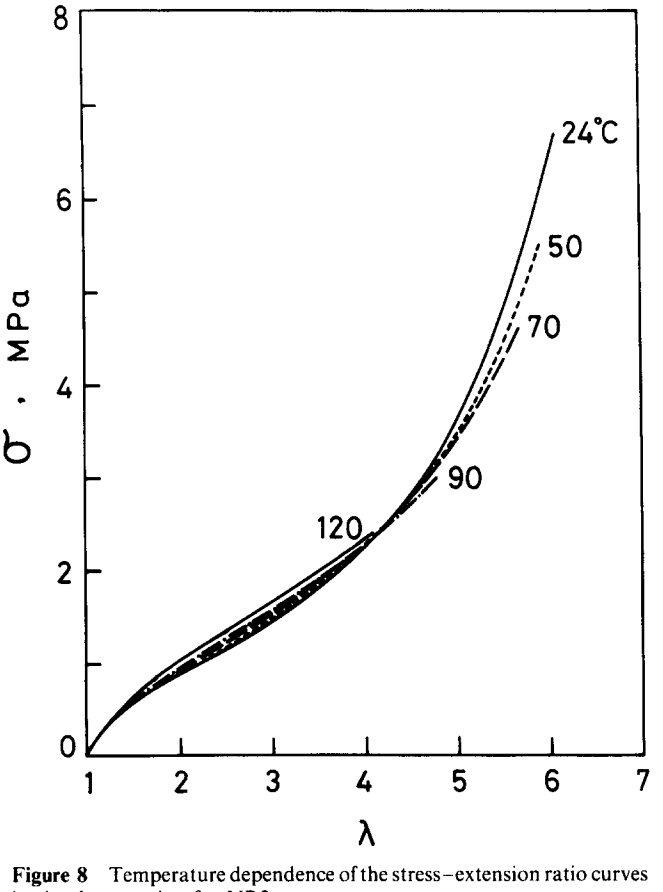

Figure 8 Temperature dependence of the stress–extension ratio curves in simple extension for NR2

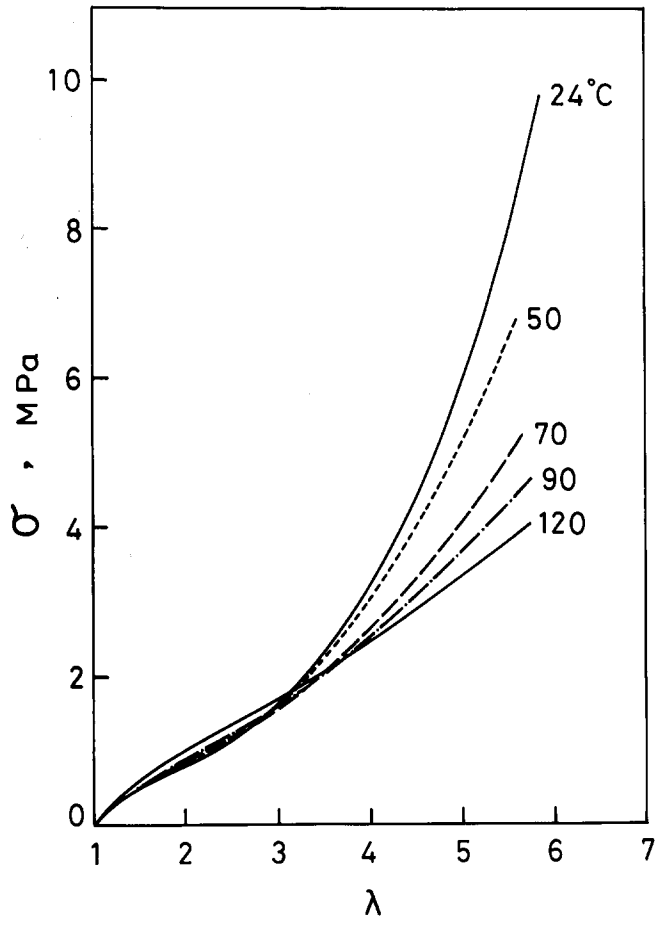

Figure 9 As *Figure 8* but for NR5

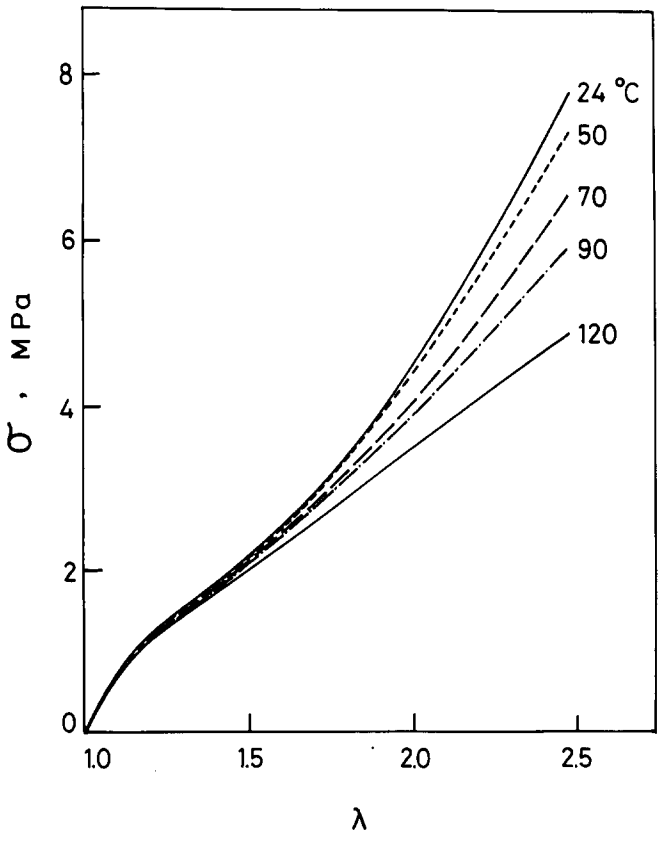

Figure 10 As *Figure 8* but for NR7

large extension but decreases at large extension as the temperature rises. Similar phenomena can also be seen in *Figure 9* for NR5. The inversion in the temperature dependence of the stress occurs at a smaller strain in *Figure 9* than in *Figure 8*, corresponding to the similar relation observed in *Figures 2* and *1*. In a heavily filled NR, the stress always decreases with increasing temperature, as shown in *Figure 10*, which is the same result as obtained in *Figure 3*. These experimental results are obviously identical to those shown on the temperature-dependent properties of $\partial W/\partial I_1$ in a wide range of extension. In the next section, therefore, we shall evaluate the entropic behaviour of rubber vulcanizates, unfilled or filled, in comparison with the theoretical derivation from the non-Gaussian theory tracing back to its original formula.

Comparison of the large-deformation behaviour of a real rubber vulcanizate and the non-Gaussian theory

The stress–extension ratio curves in simple extension theoretically predicted by equation (5) are given in *Figure 11* as a function of νkT at $n = 49$ and in *Figure 12* as a function of n at $\nu kT = 1.0$. These curves, as was

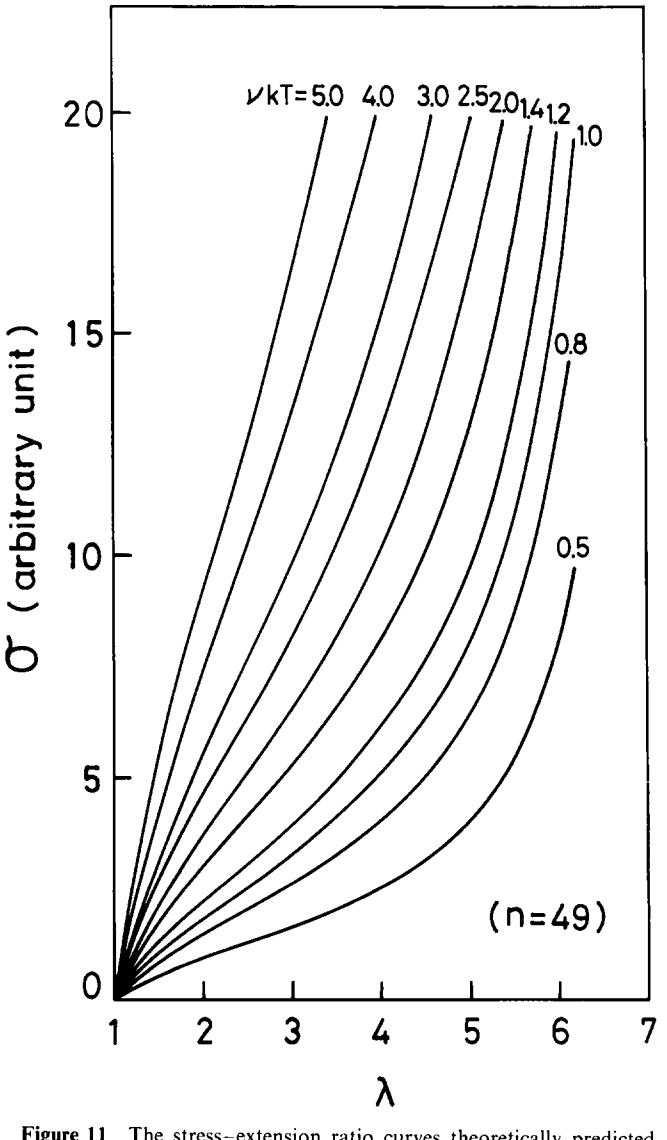

Figure 11 The stress–extension ratio curves theoretically predicted with equation (5) as a function of νkT

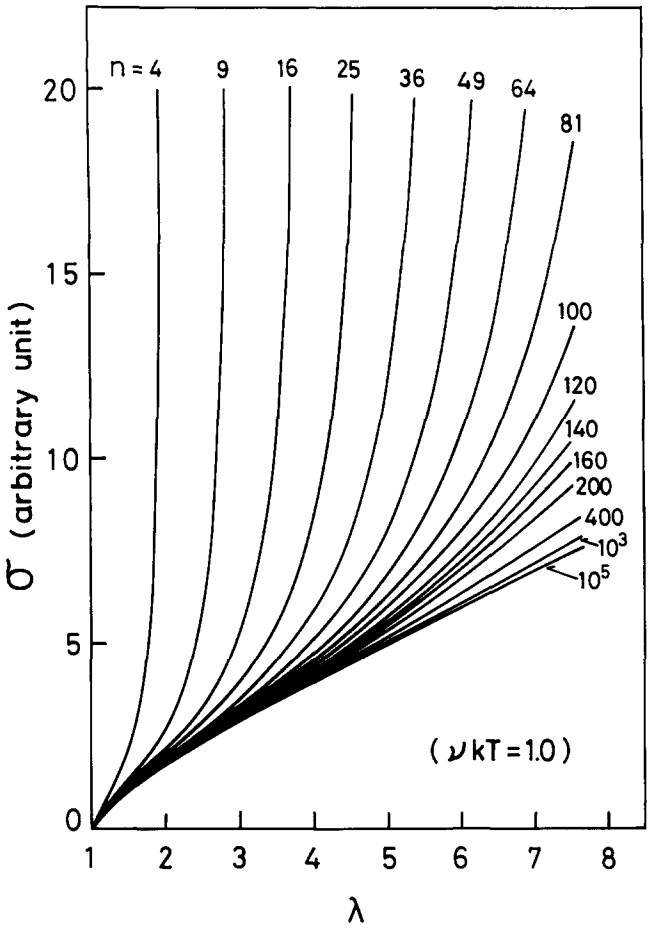

Figure 12 As *Figure 11* but as a function of n

mentioned earlier, reflect well the stress–strain behaviour of a rubber vulcanizate over a wide range of extension; particularly, they show a strong upturn at large extension. Then, comparing the stress–extension ratio curves of real rubber vulcanizates in *Figures 8*, *9* and *10* with the theoretical curves given in *Figure 12*, i.e. by picking out the theoretical curve that gives the best fit to the experimental one in each range of extension ratio, we can determine the value of n for the experimental curves as a function of λ. *Figure 13* is the value of n thus obtained at 24°C for three rubber vulcanizates. If these elastomeric materials behave in a perfect non-Gaussian way, the value of n should be constant over the whole range of extension. However, contrary to our expectations, *Figure 13* clearly shows that the value of n increases rapidly when λ exceeds some critical value λ_1, i.e. $\lambda_1 \simeq 5$ for NR2, $\lambda_1 \simeq 3$ for NR5 and $\lambda_1 \simeq 2$ for NR7. That is, molecular chains of real rubber vulcanizates, even in an unfilled NR, deviate from the non-Gaussian theory under large deformation and the deviation occurs at a smaller extension by adding fillers. *Figures 14*, *15* and *16* show the temperature dependence of the n vs. λ curves for NR2, NR5 and NR7, respectively, which indicate that the deviation from non-Gaussian behaviour occurs at a smaller extension at higher temperature.

These results tell us that a real rubber chain of an unfilled NR behaves fundamentally like a non-Gaussian chain at low temperature when extension is not large. However, at large extension, in particular at high temperature, the actual stress becomes lower compared with that calculated according to the non-Gaussian theory, which we have interpreted as an increase of n and thus a decrease of ν (because $n\nu$ = constant) up to this point in the present paper. The stress decrease occurs more clearly in a filled NR. Consequently, to understand these phenomena, we must consider an unstable or unfixed crosslink in a real rubber chain network, which can change its properties according to deformation conditions, such as strain amplitude, temperature and velocity. These developments could just be derived by evaluating the molecular behaviour of elastomers under a very large extension. In the next section, we propose a new model that will be able to explain the above phenomena and the temperature-dependent properties of the stress–strain curve discussed above, as well as the hysteresis properties of real rubber vulcanizates.

DISCUSSION

Interpretation of molecular behaviour of rubber chain networks with the new slider model

Now we consider the first assumption that there are two types of crosslink, chemical and physical, in real rubber vulcanizates, whose numbers are ν_c and ν_p respectively, with $\nu = \nu_c + \nu_p$. Physical crosslinks as

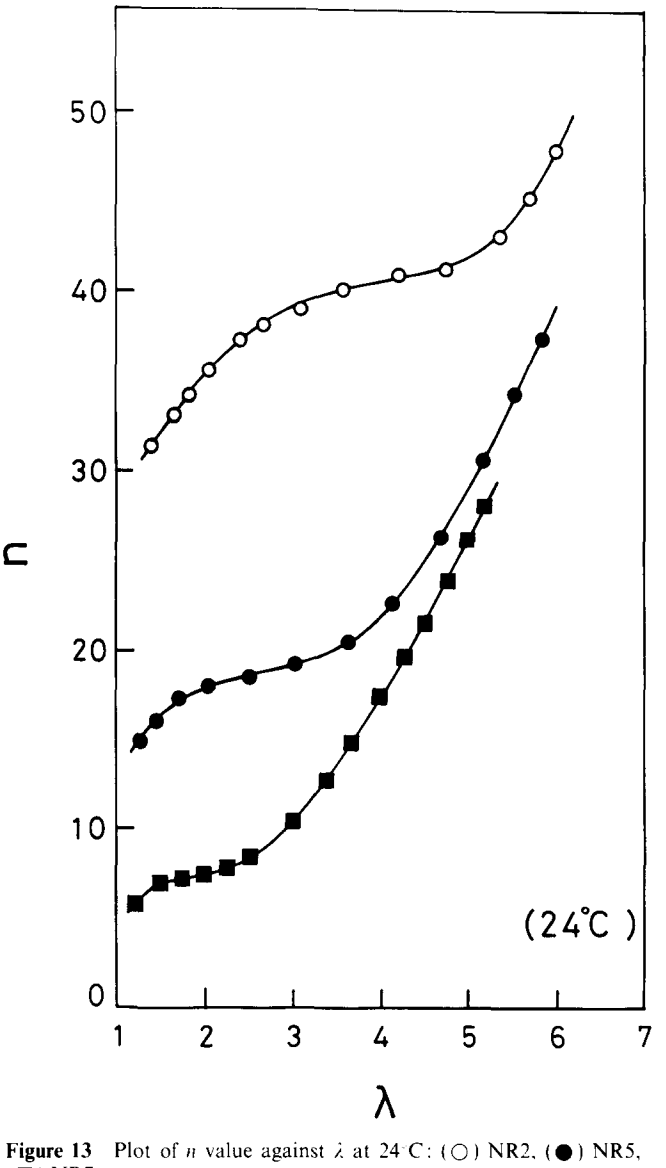

Figure 13 Plot of n value against λ at 24°C: (○) NR2, (●) NR5, (■) NR7

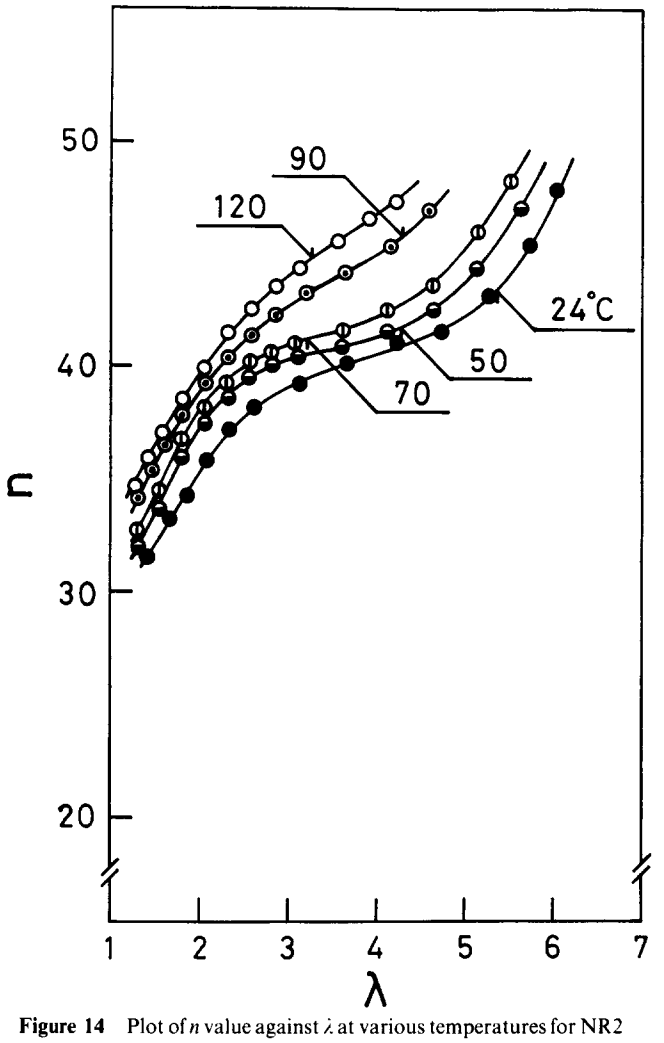

Figure 14 Plot of n value against λ at various temperatures for NR2

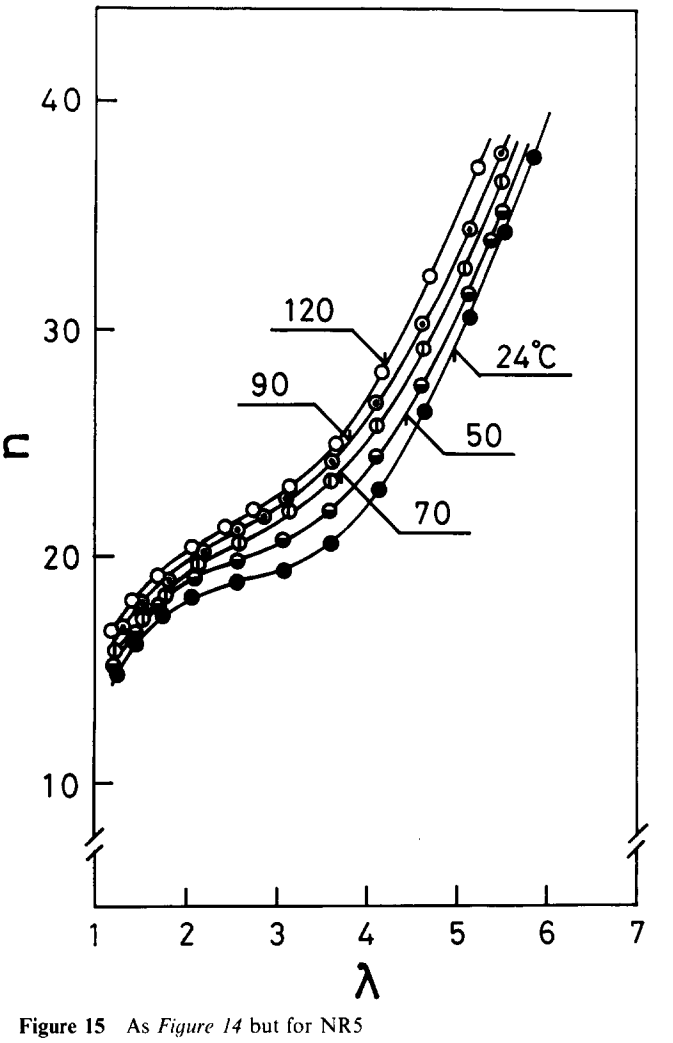

Figure 15 As *Figure 14* but for NR5

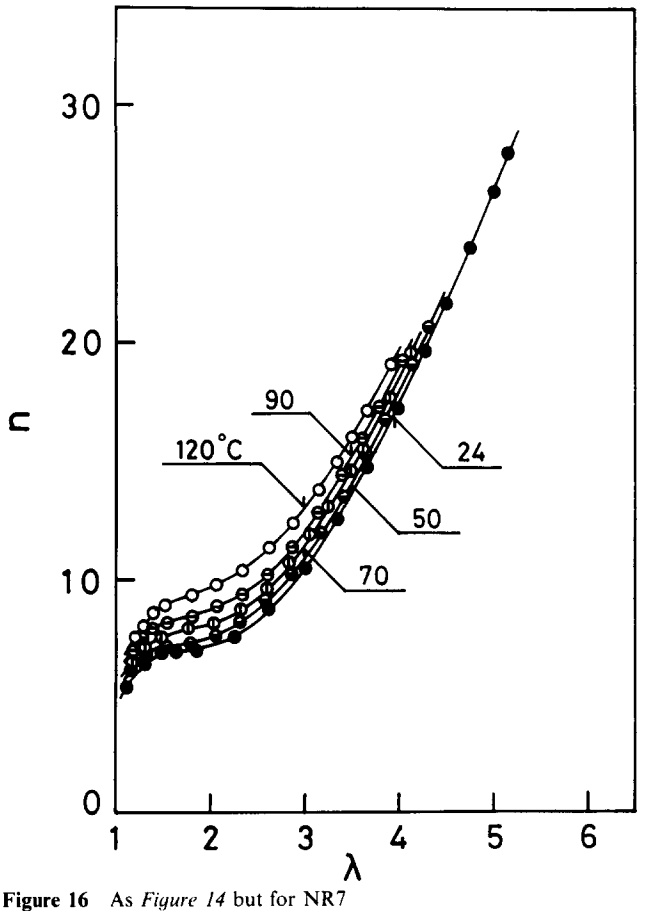

Figure 16 As *Figure 14* but for NR7

defined here include all types of crosslinks except chemical crosslinks, which are, in other words, the segment–segment interaction junctions adhered to each other by molecular attractive forces. The bonding strength of the interaction in physical crosslinks is much weaker than that of chemical crosslinks, and as a result the slippage back and forth of segments along a molecular chain occurs easily in physical crosslinks due to external forces, as schematically represented in *Figure 17*.

We give the following frictional sliding model for physical crosslinks. The slider is connected to a spring and fixed to the object. The slider does not move when the tension F is smaller than a critical magnitude F_0 and begins to move at $F \geqslant F_0$. The friction mode varies from static to kinetic in this process.

Here, we set up a parallel combination of a spring and a slider which is, to be exact, connected in series to another spring. The former corresponds to chemical crosslinks and the latter to physical crosslinks, shown in *Figure 18*. The stress–strain curve is given by curve A in *Figure 19* for a spring and curve B for a slider. Then half of the combination of curves A and B will produce curve C (*Figure 19*), taking into account that there should be many types of distribution in the distance between physical crosslinks and in the magnitude of bonding strength. When the extension ratio is smaller than a critical value λ_0, all crosslinks, with no difference between chemical and physical, behave as fixed crosslinks. In the vicinity of the critical extension ($\lambda \simeq \lambda_0$), physical

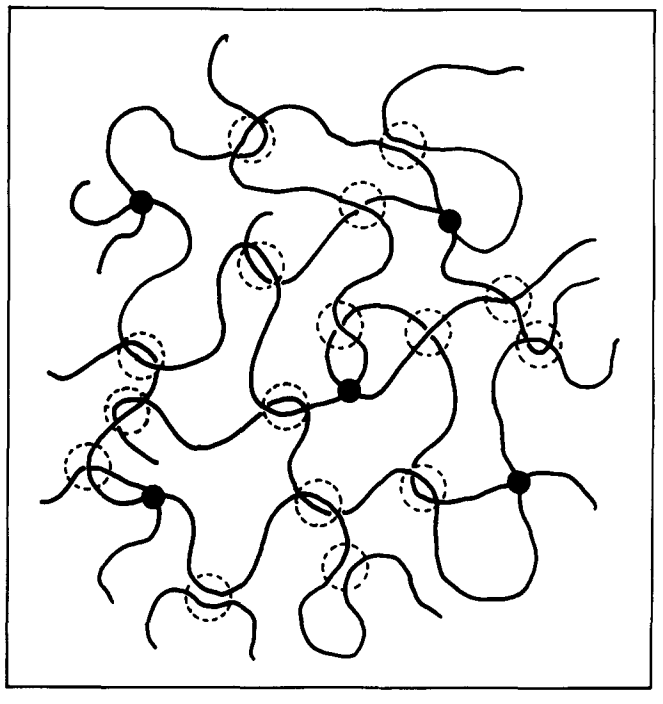

Figure 17 Molecular structures (schematic): black dots represent chemical crosslinks; broken circles are physical crosslinks

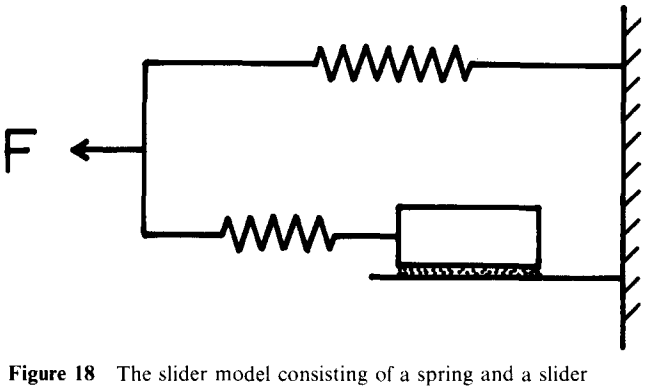

Figure 18 The slider model consisting of a spring and a slider

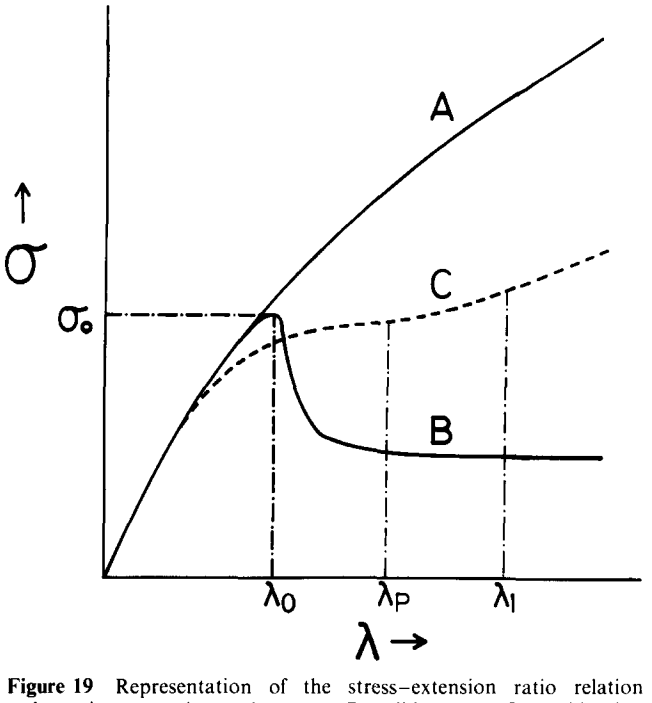

Figure 19 Representation of the stress–extension ratio relation (schematic): curve A, a spring; curve B, a slider; curve C, combination of a spring and a slider

crosslinks gradually change their friction modes from static to kinetic, following which they begin to slide with the coefficient of kinetic friction μ_k. Most of the physical crosslinks will slide at larger extension ($\lambda > \lambda_0$), and as a result the stress will be lower than that expected according to the non-Gaussian theory based on the assumption that all crosslinks are fixed. In brief, the deviation of the stress–strain relation in a real rubber chain from a non-Gaussian behaviour is based on the fact that physical crosslinks change their frictional properties from static to kinetic with increasing extension, and consequently the stress becomes lower because $\mu_k < \mu_s$, i.e. $\sigma_k < \sigma_s$.

Let us now return to the initial question of why the stress–strain curves measured at different temperatures cross each other at medium extension. Here we make the second assumption that the friction coefficient of the slider introduced above has viscous properties, that is the friction coefficient of the slider depends on temperature and velocity. *Figure 20* gives the temperature dependence of the static and kinetic friction coefficients measured between natural rubber (NR2) and an iron stick, with representative results[23] superimposed on the experimental data. The value of μ_k is nearly a half of μ_s at 20°C and a third of μ_s at 100°C and both μ_k and μ_s decrease gradually as the temperature increases.

Now we consider the stress–strain curves at 20 and 100°C. Although the stress is 1.27 times higher at 100°C than at 20°C owing to the entropic contribution in the range of small strain, the increase in stress at 100°C will be cancelled by the lowering of the stress caused by a decrease of the kinetic friction coefficient at 100°C, i.e. $\mu_k(100°C)/\mu_k(20°C) = 0.50$ at larger strain given in *Figure 20*. Therefore, if the contribution from slider elements is higher than that from spring elements, and in fact the number of slider elements seems to be much higher than the number of spring elements, the stress at 100°C will be lower than that at 20°C, producing the crossing of the stress–strain curves. As a result, the crossing will occur at smaller extension the more the system includes physical crosslinks. In filled rubber vulcanizates, there must be a tremendous number of slider elements, and in addition sliders generate heat and

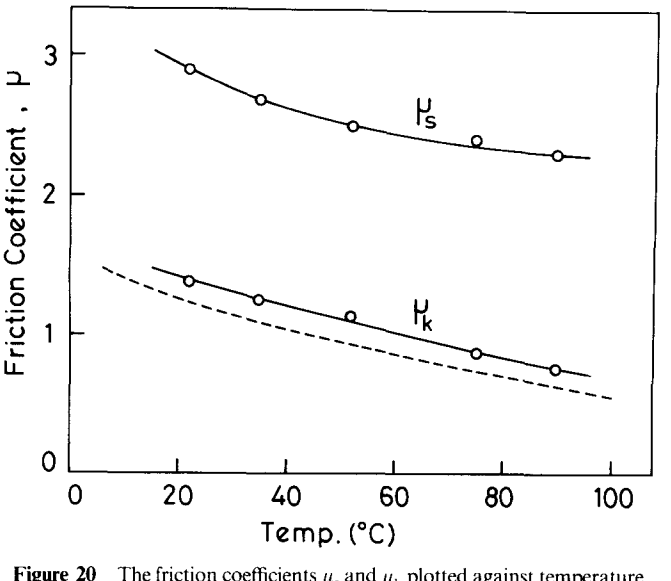

Figure 20 The friction coefficients μ_s and μ_k plotted against temperature. Also shown for reference are representative results[23] for μ_k (------)

raise the local temperature, which produces a drastic decrease of stress in the stress–strain relation and the curves of $(\partial/\partial T)(\partial W/\partial I_1)$ vs. I_1 as discussed before. We have confirmed the validity of the slider model for understanding the molecular behaviour of elastomers in this section. As the next item for discussion, we would like to apply the slider model to analyse some other phenomena observed in rubber.

Analysis of the Mullins effect by the slider model

One of the most characteristic and interesting phenomena in rubber vulcanizates is an irreversible stress softening called the Mullins effect[24], which should be a suitable subject to evaluate the intrinsic value of the new slider model. When rubber is extended to λ_p, returned to $\lambda = 1$ and extended again, the second stress–strain curve lies below the first one, but rejoins at λ_p (*Figure 21*). Although this phenomenon occurs even in unfilled rubber vulcanizates, it increases greatly in carbon-black-filled rubber vulcanizates. There have been various mechanisms proposed to explain the Mullins effect, for example fracture of network chains[25], chain detaching from the surface of filler particles[26,27] and chain crystallization[28]. In the absence of these phenomena, of course, the reduction in stress during unloading of a rubber network is credited to viscoelastic softening, i.e. retardation in the response of network chains due to interaction with the surrounding viscous medium[29]. However, the stress softening due to linear viscoelasticity calculated by taking into consideration the relaxation time of a material comparable to the time-scale of deformation is much less than the actual hysteresis, nearly half of the Mullins softening[30].

Now let us analyse the Mullins effect using the new slider model. First, we would like to explain the relation between the stress softening due to linear viscoelasticity and the Mullins softening. In the model given in *Figure 18*, since the friction force of a sliding element works in the opposite direction to the tension F in loading, the stress of the system, σ_l, is given by the sum of the stress produced by each element, namely chemical crosslink, σ_c,

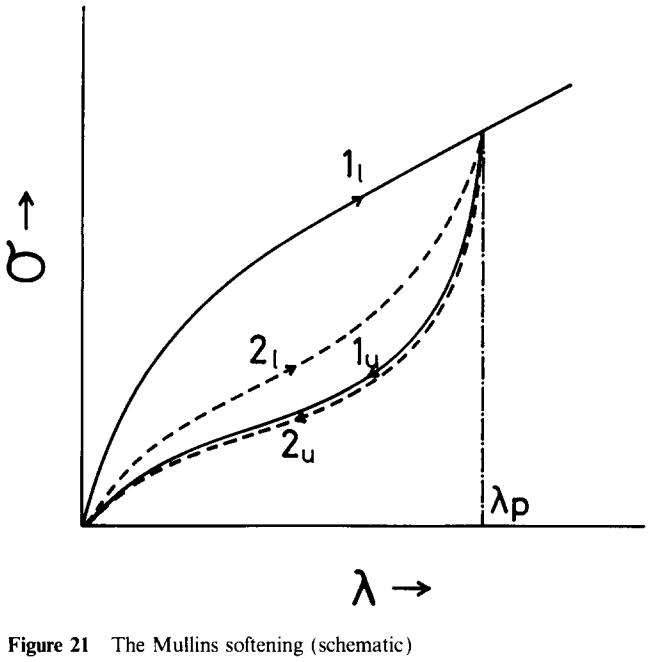

Figure 21 The Mullins softening (schematic)

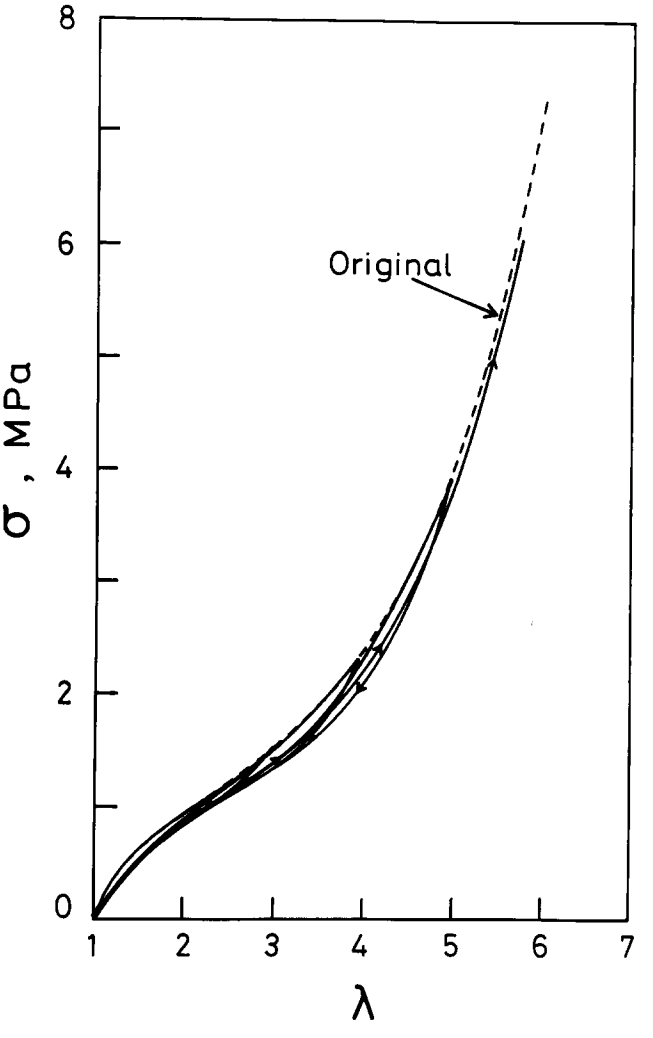

Figure 22 The Mullins softening for NR2

and physical crosslink (static and kinetic), σ_{ps} and σ_{pk}, that is:

$$\sigma_l = \sigma_c + \sigma_{ps} + \sigma_{pk}$$

In unloading, however, when a sliding element moves in the opposite direction, the friction force of a sliding element works in the same direction as the tension F, and consequently the stress of the system, σ_u, is given by:

$$\sigma_u = \sigma_c + \sigma_{ps} - \sigma_{pk}$$

As a result, the difference in stress in loading and unloading, $\Delta\sigma$ $(= \sigma_l - \sigma_u)$, will be given as $2\sigma_{pk}$, that is, the Mullins softening will be about twice as large as the viscoelastic softening.

Another characteristic of the Mullins softening is that the second loading curve lies between the first loading and unloading curves and the second unloading curve lies below the second loading curve, and after the second cycle the hysteresis loop scarcely changes its shape, as shown in *Figure 21*. This phenomenon can be explained by considering the temperature rise in a slider during sliding both ways, which will be nearly constant after repeated cycles.

Figures 22, *23* and *24* are the Mullins softening of NR2, NR5 and NR7, respectively. When the extension ratio exceeds λ_1, the stress should quickly return to the original stress–strain curve. In fact, the stress joins up to the original curve with some time delay due to a temperature

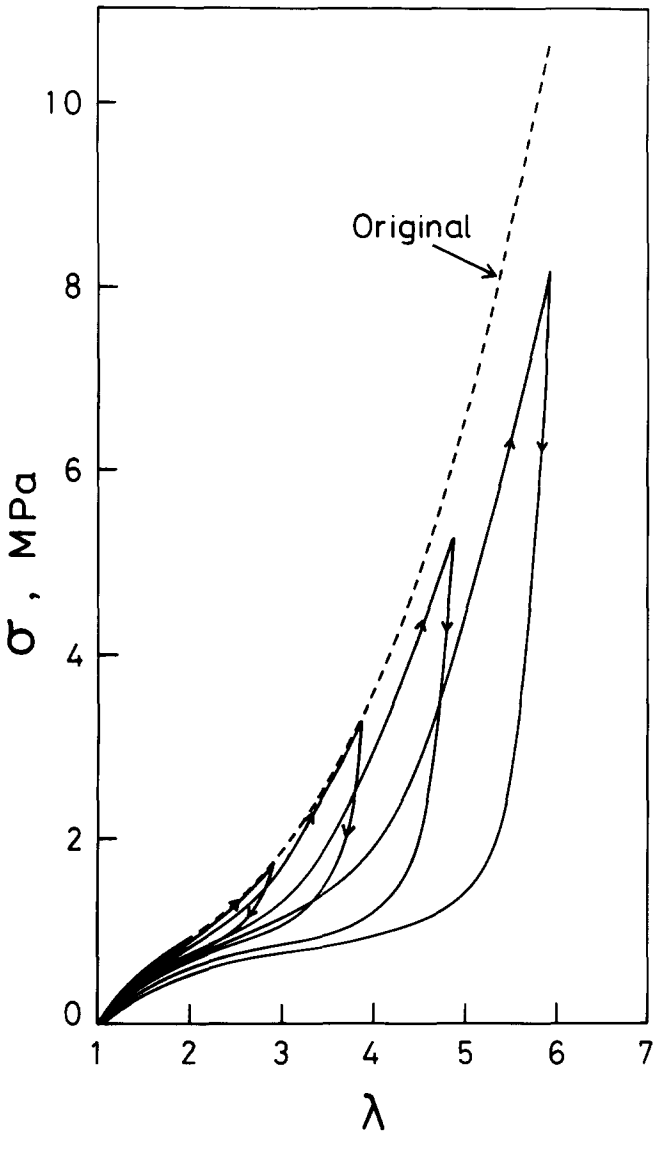

Figure 23 As *Figure 22* but for NR5

rise, which of course produces the reduction of the friction coefficients μ_s and μ_k.

Molecular behaviour of a rubber chain network under large extension and retraction

As a first step, we consider the molecular behaviour of rubber chain networks using the concept given by the slider model. The most important point of the new slider model is its viscous property, i.e. the friction coefficients μ_s and μ_k depend on temperature T and velocity v, and thus are given by $\mu_s(T, v)$ and $\mu_k(T, v)$. Moreover, since the sliding of molecular chains causes a temperature rise first in a local region and then spreading all over the system, the strain amplitude also governs μ_k, so $\mu_k(T, v, \lambda)$.

Now we make the assumption that any type of physical crosslink consists of an adhesive junction of two adjacent molecular segments and its bond strength depends on the distance between segments: the shorter the distance, the stronger the bonding (*Figure 25a*). In the case of carbon-black-filled rubber, we assume a strong interaction between rubber chain and carbon black, in which the absorption of molecular segments at several sites of a filler surface introduces giant multifunctional crosslinks into the system; thus there is a significant increase of the crosslink density, schematically shown in *Figure 25b*. Now we consider the molecular mechanism of a rubber chain network in relation to the stress–strain relation given by *Figure 19*, in which curve A corresponds to the case where all crosslinks are chemical crosslinks

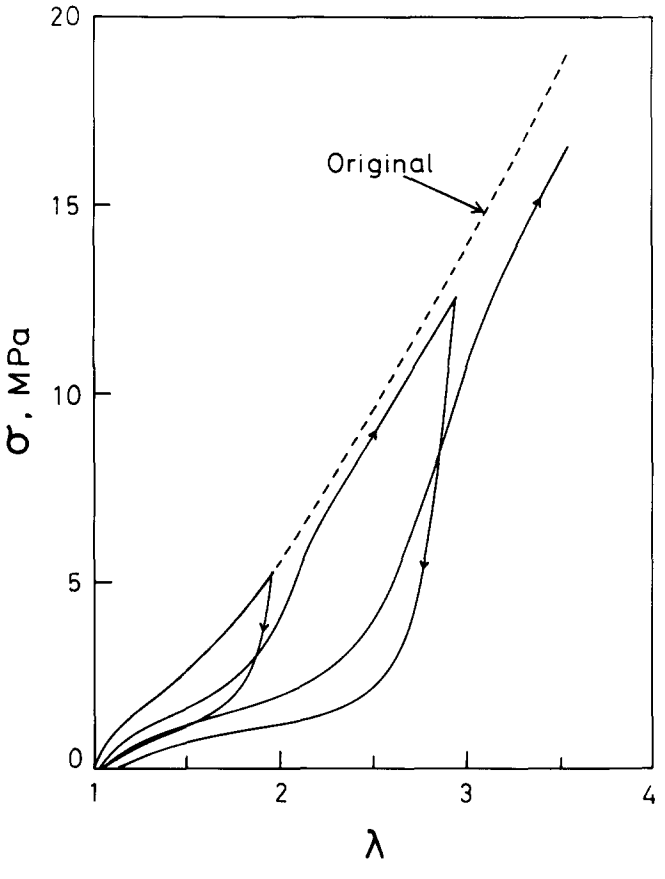

Figure 24 As *Figure 22* but for NR7

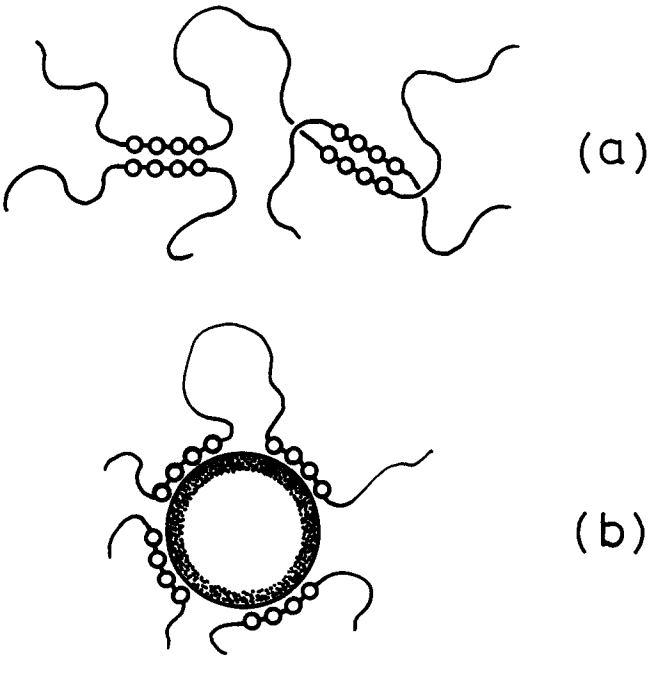

Figure 25 Physical crosslinks (schematic): (a) two adjacent molecular segments; (b) multifunctional crosslinks between rubber chain and carbon black

and curve C to that consisting of both chemical and physical crosslinks. In the region of small extension $1 \leqslant \lambda \leqslant \lambda_0$ where physical crosslinks are fixed at crosslink junctions like chemical crosslinks, all dynamic behaviour is reversible. When physical crosslinks begin to slide at $\lambda \geqslant \lambda_0$, the segment–segment distance becomes wider due to the local temperature rise and as a result curve C deviates more from curve A with increasing extension. During cyclic deformation at $\lambda = \lambda_p$ within such a region, the segment–segment distance will remain nearly constant, because even if the local temperature becomes lower during unloading, it seems to take a long time for re-narrowing of the distance to occur at lower temperature.

When extension exceeds another critical point $\lambda = \lambda_1$, debonding or detaching will occur at the adhesive junction of two adjacent segments and at the interface between rubber chain and filler. Even breakage of rubber chains or fillers will occur in an extreme case, in addition to the increase of the segment–segment distance. These structural changes decrease the effective number of crosslinks, which can be seen on *Figure 13* or *Figures 14, 15* and *16*, as was discussed before. This critical extension λ_1 seems to be identical to the extension at which the second loading curve does not join up to the original curve, shown in *Figures 22, 23* and *24*, respectively. An irreversible permanent set will be produced after such a large deformation.

CONCLUSIONS

The plots of $\partial W/\partial I_1$ vs. I_1 and the stress–strain curves in simple extension measured at different temperatures for real rubber vulcanizates cross each other at medium extension. A stress increase proportional to absolute temperature is only seen in a range of small to medium extension, and this relation reverses itself at large extension, which seems to be closely associated with deviation from the non-Gaussian theory based on the concept of fixed crosslinks.

We have proposed a new slider model, in which a slider with the characteristic viscous property is introduced to represent physical crosslinks of real materials. The slider model is effectively available for interpreting not only the above phenomena but also the Mullins softening observed under cyclic deformation.

REFERENCES

1 Mark, J. E. *Adv. Polym. Sci.* 1982, **44**, 1
2 Erman, B., Wagner, W. and Flory, P. J. *Macromolecules* 1980, **13**, 1554
3 Flory, P. J. and Erman, B. *Macromolecules* 1982, **15**, 800
4 Erman, B. and Flory, P. J. *Macromolecules* 1982, **15**, 806
5 Dossin, L. M. and Graessley, W. W. *Macromolecules* 1979, **12**, 123
6 Pearson, D. S. and Graessley, W. W. *Macromolecules* 1980, **13**, 1001
7 Gottlieb, M., Macosko, C. W. and Lepsch, T. C. *J. Polym. Sci., Polym. Phys. Edn.* 1981, **19**, 1603
8 Doi, M. and Edwards, S. F. *J. Chem Soc., Faraday Trans. (II)* 1978, **74**, 1789, 1802, 1818
9 Ball, R. C., Doi, M., Edwards, S. F. and Warner, Z. M. *Polymer* 1981, **22**, 1010
10 Gottlieb, M., Macosko, C. W., Benjamin, G. S., Meyers, K. O. and Merrill, E. W. *Macromolecules* 1981, **14**, 1039
11 Fukahori, Y. and Seki, W. *Polymer* 1992, **33**, 502
12 Meyer, K. H., von Susich, G. R. and Valko, E. *Kolloid Z.* 1932, **59**, 208
13 Kuhn, W. *Kolloid Z.* 1934, **68**, 2; 1936, **76**, 258
14 James, M. H. and Guth, E. *J. Chem. Phys.* 1943, **11**, 455
15 Flory, P. J. *J. Chem. Phys.* 1950, **18**, 108
16 Flory, P. J. *Proc. R. Soc. Lond. (A)* 1976, **351**, 351
17 Graessley, W. W. *Macromolecules* 1975, **8**, 186, 865
18 Flory, P. J. *Polymer* 1979, **20**, 1317
19 Shen, M. *Macromolecules* 1969, **2**, 358
20 Kawabata, S., Matsuda, M. and Kawai, H. *Macromolecules* 1981, **14**, 154
21 Kuhn, W. and Grün, F. *Kolloid Z.* 1942, **101**, 248
22 Treloar, L. R. G. 'Physics of Rubber Elasticity', Oxford University Press, London, 1958
23 Grosch, K. A. *Proc. R. Soc. Lond. (A)* 1963, **274**, 21
24 Mullins, L. and Tobin, N. R. *Rubber Chem. Technol.* 1957, **30**, 555
25 Huang, W. N. and Aklonis, J. J. 'Chemistry and Properties of Crosslinked Polymers' (Ed. S. S. Labana), Academic Press, New York, 1977, p. 453
26 Bueche, F. 'Physical Properties of Polymers', Wiley, New York, 1962, p. 49
27 Sato, R. *Nippon Gomu Kyokai Shi* 1964, **37**, 99
28 Harwood, J. A. C. and Payne, A. R. *J. Appl. Polym. Sci.* 1967, **11**, 1825
29 Mullins, L. *Rubber Chem. Technol.* 1969, **42**, 339
30 Roland, C. M. *Rubber Chem. Technol.* 1989, **62**, 880